Supplementary Information (SI) for Journal of Materials Chemistry C.

High-Sensitivity Indirect X-ray Detector Using Ultrasonically Exfoliated MoS_2 Monolayer in active layer

Chanyeol Lee, [a] Jehoon Lee[b], Jaewon Son [a] and Jungwon Kang [*c, d]

[a.] Department of Foundry Engineering, Dankook University, Yongin-si 16890, Korea

[b.] Device Enabling Team, DB HiTek Bucheon-si 14519, Korea

[c.] Convergence Semiconductor Research Center, Dankook University, Yongin-si 16890, Korea

[d.] Department of Convergence Semiconductor Engineering, Dankook University, Yongin-si 16890, Korea

*Correspondence: jkang@dankook.ac.kr (J.K.)

1. Images of MoS_2 after exfoliation and centrifugation and developed X-ray detector.

When MoS_2 is dispersed in DMF, the color changes from dark gray to increasingly yellow as the centrifugation speed increases.

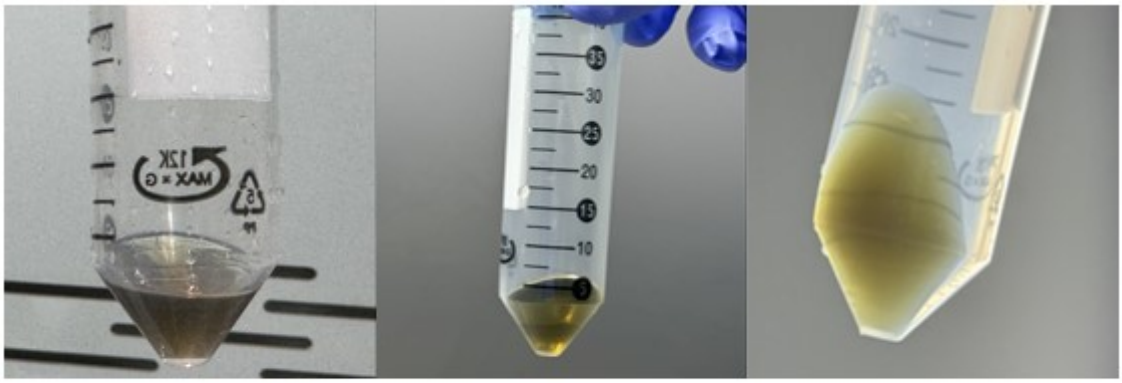

Fig. S1 MoS_2 centrifugated by a) 4000 rpm, b) 6000 rpm, c) 8000 rpm after exfoliation.

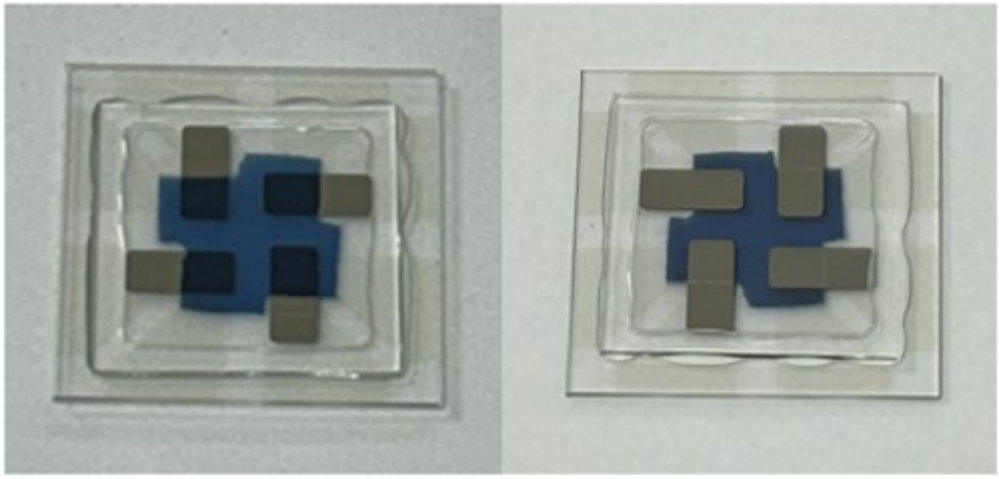

Fig. S2 Images of a) front side and b) back side of developed X-ray detector

2. Photovoltaic parameters of developed X-ray detector.

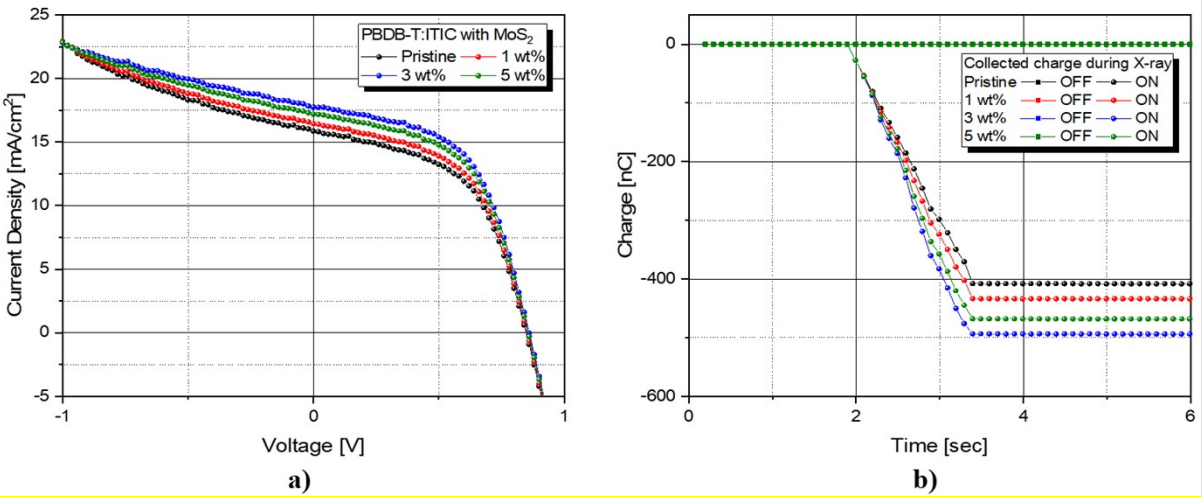

Fig. S3 Photovoltaic parameters of PBDB-T:ITIC devices with different MoS_2 concentrations. a) J-V curve according to different concentration of MoS_2 with solar simulator. b) Collected charge of detectors based on PBDB-T:ITIC active layer with different concentration of MoS_2

Table S1. Photovoltaic parameters and X-ray detecting characteristics among MoS_2 content

Content of MoS_2	EFF [%]	J_{SC} [mA/cm2]	V_{OC} [mV]	R_S [Ω]	Sensitivity [mA/Gy·cm^2]	CCD-DCD [μA/cm^2]
Pristine	6.07 ± 0.20	15.86 ± 0.24	847.76 ± 10	489 ± 14	1.440	4.82
1 wt%	6.42 ± 0.16	16.43 ± 0.56	851.32 ± 9	457 ± 11	1.549	5.19
3 wt%	7.13 ± 0.11	17.76 ± 0.26	859.61 ± 12	376 ± 13	1.804	6.04
5 wt%	6.79 ± 0.13	17.21 ± 0.11	856.06 ± 12	421 ± 15	1.702	5.67

Based on the Fig. S3 and Table S1, we determined the MoS_2 content to be 3 wt%. Using 1 wt% MoS_2 would be too low, resulting in minimal effect. Adding 5 wt% MoS_2 would be excessive, potentially affecting the BHJ structure between PBDB-T and ITIC and hindering charge transport.

Table S2. Photovoltaic parameters including R_{SH}, FF of developed X-ray detectors

Size of MoS_2	EFF [%]	FF [%]	J_{SC} [mA/cm^2]	V_{OC} [mV]	R_S [Ω]	R_{SH} [Ω]
Pure	6.07	51.9	15.86	847.7	489	9154
Bulk MoS_2	6.53	52.2	16.62	855.9	469	7020
70 nm	6.68	52.6	17.15	848.6	449	9980
40 nm	7.03	52.8	17.53	868.3	415	5540
25 nm	7.13	53.0	17.76	859.6	376	7630
17 nm	6.75	52.9	16.79	858.2	458	8053

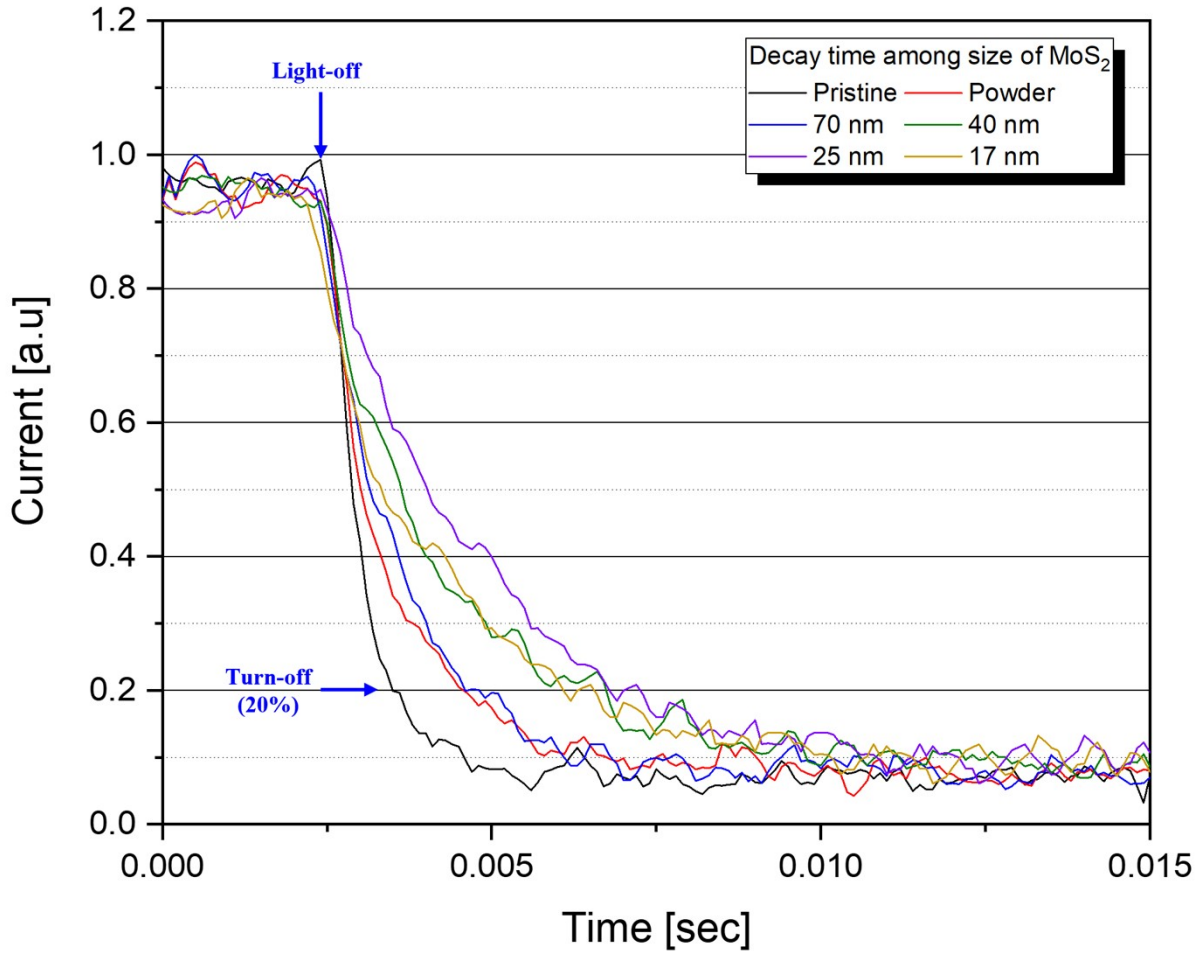

Fig. S4 Decay time among size of MoS_2 for extracting effective carrier lifetime

Considering the dark current, the turn-off point is defined as the point where the device current reaches 20%. The decay times for pristine, powder, 70 nm, 40 nm, 25 nm, and 17 nm devices are 0.0035, 0.0046, 0.0049, 0.0066, 0.0073, and 0.0068 seconds, respectively. These decay times are similar to the carrier lifetimes calculated using the Langevin recombination model, with the device with 25 nm MoS_2 exhibiting the highest performance.

Table S3. Thickness deviation of PBDB-T:ITIC active layer among MoS_2 size

Size of MoS_2	Pristine	70 nm	40 nm	25 nm	17 nm
Thickness [nm]	95±2	103±4	101±3	97±2	96±2

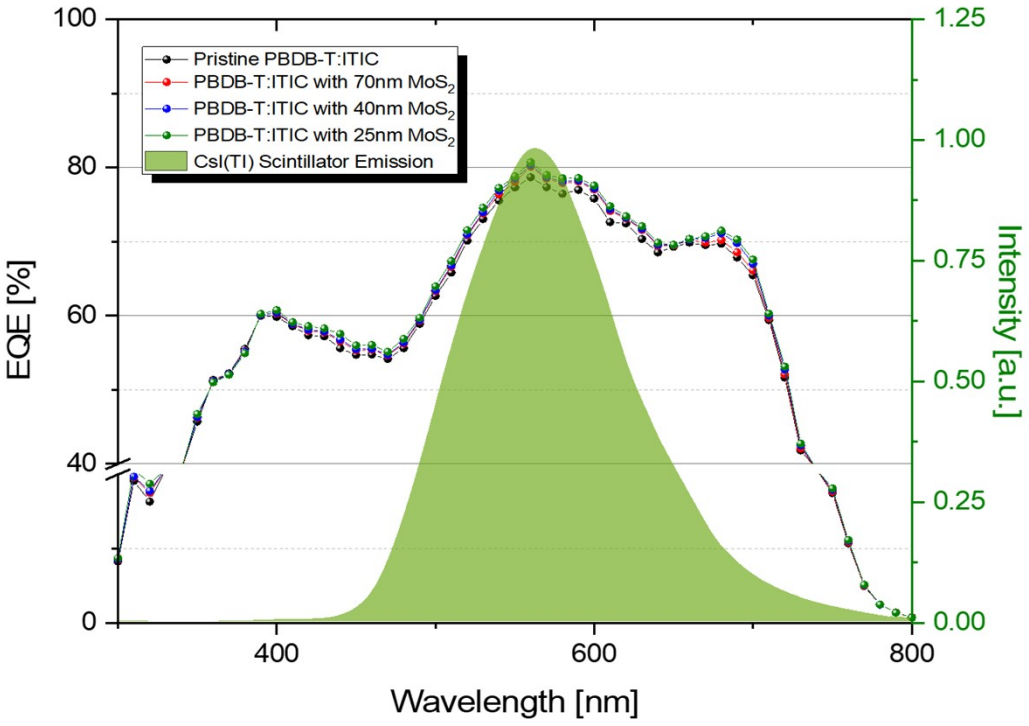

Fig. S5 EQE of PBDB-T:ITIC devices with different size of MoS_2

3. AFM images of active layer of X-ray detector

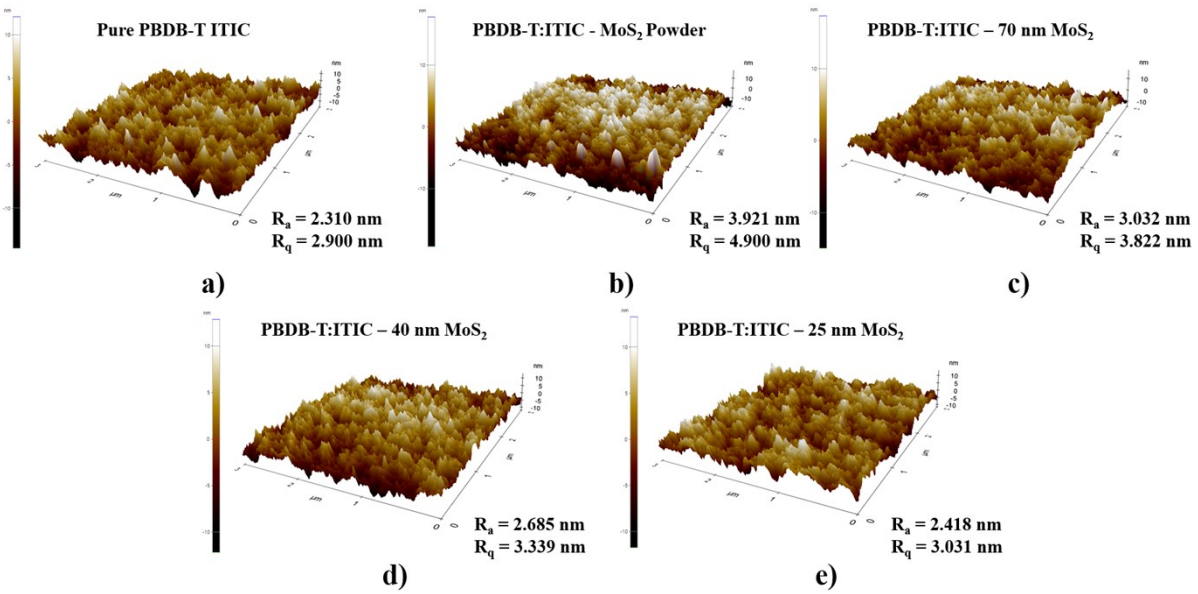

Fig. S6 AFM images of a) Pure PBDB-T:ITIC and PBDB-T:ITIC with b) powder, c) 70 nm. d) 40 nm, e) 25 nm size of MoS_2